Preprints.org

Article

Not peer-reviewed version

Development of n-type, Passivating Nanocrystalline Silicon Oxide (nc-SiOx:H) Films via PECVD

Gurleen Kaur * , Antonio J. Olivares , Pere Roca i Cabarrocas *

Posted Date: 20 February 2024

doi: 10.20944/preprints202402.1053.v1

Keywords: nanocrystalline silicon oxide, "nc:SiOx:H"; n-type; surface passivation; amorphous silicon; PECVD; effective carrier lifetime

Preprints.org is a free multidiscipline platform providing preprint service that is dedicated to making early versions of research outputs permanently available and citable. Preprints posted at Preprints.org appear in Web of Science, Crossref, Google Scholar, Scilit, Europe PMC.

Copyright: This is an open access article distributed under the Creative Commons Attribution License which permits unrestricted use, distribution, and reproduction in any medium, provided the original work is properly cited.

Preprints.org (www.preprints.org) | NOT PEER-REVIEWED | Posted: 20 February 2024

doi:10.20944/preprints202402.1053.v1

Disclaimer/Publisher's Note: The statements, opinions, and data contained in all publications are solely those of the individual author(s) and contributor(s) and not of MDPI and/or the editor(s). MDPI and/or the editor(s) disclaim responsibility for any injury to people or property resulting from any ideas, methods, instructions, or products referred to in the content.

Article

Development of n-Type, Passivating Nanocrystalline Silicon Oxide (nc-SiOx:H) Films via PECVD

Gurleen Kaur [1,2,*], Antonio J. Olivares [2] and Pere Roca i Cabarrocas [1,2,*]

[1] Institut Photovoltaïque d'Ile-de-France (IPVF), 18 Bvd Thomas Gobert, 91120 Palaiseau, France
[2] LPICM, CNRS, Ecole Polytechnique, Institut Polytechnique de Paris, route de Saclay, 91128 Palaiseau, France
* Correspondence: gur.khera@gmail.com; pere.roca@polytechnique.edu

Abstract: Nanocrystalline silicon oxide (nc-SiOx:H) is a multipurpose material with its varied application in solar cells as a transparent front contact, intermediate reflector, back reflector layer and even tunnel layer for passivating contacts, owing to easy tailoring of its optical properties. In this work, we systematically investigate the influence of gas mixture (SiH_4, CO_2, PH_3 and H_2), RF power and process pressure on the optical, structural and passivation properties of thin n-type nc-SiOx:H films prepared in an industrial, high throughput, plasma-enhanced chemical vapor deposition (PECVD) reactor. We provide a detailed description of the n-type nc-SiOx:H material development using various characterization techniques (SEM, EDX, Raman spectroscopy, and spectroscopic ellipsometry) with a focus on the relationship between the material properties and the passivation they provide to n-type c-Si wafers characterized by their effective carrier lifetime (τ_{eff}). Further, we also outline the parameters to be kept in mind while developing different n-type nc-SiOx:H layers for different solar cell applications. We report a tunable optical gap (1.8 – 2.3 eV) for our n-type nc-SiOx:H films as well as excellent passivation properties with τ_{eff} up to 4.1 ms (iV_{oc} ~ 715 mV) before annealing. Oxygen content plays an important role in determining the crystallinity and hence passivation quality of the deposited nanocrystalline silicon oxide films.

Keywords: nanocrystalline silicon oxide; nc:SiOx:H; n-type; surface passivation; amorphous silicon; PECVD; effective carrier lifetime

1. Introduction

In past decade nanocrystalline silicon oxide (nc-SiOx:H) films as a functional multipurpose material has garnered significant interest of the photovoltaic community [1–4]. This is due to its broad range of optical and electrical properties, which can be tuned by varying deposition parameters: i.e. absorption coefficient, refractive index, optical band gap, and p-type and n-type doping which allow to make selective contacts. Doping of films with phosphorus (n-type) has resulted in further improved conductivities, and hydrogen atoms in the mixture have resulted in effective defect passivation [5]. Nanocrystalline silicon oxide (nc-SiOx:H) consists of crystalline silicon nanoparticles embedded in an amorphous phase composed of silicon oxide (a-SiOx:H) and a-Si:H phases [6,7]. The two-phase structure of nc-SiOx:H materials has been suggested to help achieve a large optical gap while keeping a high conductivity. The oxygen-rich Si-O-Si phase of the material helps to increase the optical gap and decrease the refractive index, while the Si-rich portion of the material via an intricate three-dimensional network of crystallites is known to provide high electrical conductivity pathways both in lateral and transverse directions [8].

The research on nc-SiOx:H layers was first developed for single junction μc-Si:H solar cells. It provided better light trapping and acted as a good window layer [4,9,10,11]. By using a suitable bilayer of two crystalline SiOx:H layers (as n layer as well as back reflector) solar cell efficiencies improved in p-i-n structure based single junction solar cells [12]. Later on, the material was applied to silicon heterojunction (HJT) solar cells – on both textured and flat substrates, where nanocrystalline silicon oxide layer (nc-SiOx:H) has been used as a wide-gap window layer instead of a-Si:H layer [13,14]. Compared with a-Si:H layers n-type nc-SiOx:H offer higher transparency, similar electrical conductivity and lower refractive index. Mazzarella et al. also studied the use of ~ 5 nm thick n-type

© 2024 by the author(s). Distributed under a Creative Commons CC BY license.

Preprints.org (www.preprints.org) | NOT PEER-REVIEWED | Posted: 20 February 2024 doi:10.20944/preprints202402.1053.v1

nc-SiOx:H as front contacts (exhibiting high front surface field) in rear-emitter SHJ solar cells resulting in efficiencies of 22.6% [15]. The use of nc-SiOx as electron transport layer has subsequently improved the power conversion efficiency to 23.1% (V_{oc} = 738 mV, J_{sc} to 39 mA cm^{-2}) [16].

Doped nc-SiOx:H layers also have dual application in tandem thin films solar cells – (i) as an intermediate reflector between the the n/p recombination junction (i.e. a-Si:H and μc-Si:H) because of a step in refractive index and (ii) as n-layer of the μc-Si:H bottom cell to reduce parasitic absorption [6,10,17]. The application of n-type and p-type nc-SiOx:H as a FSF layer and rear-emitter layer resulted in a textured rear-emitter SHJ solar cell with efficiency of 21.4% [8]. Even poly-Si layers in TOPCon solar cells have been replaced by ultrathin nc-SiOx:H to enhance transparency [18,19]. Further, nc-SiO_x layers have demonstrated clear advantages for maximizing the infrared response of c-Si bottom cells in combination with perovskite top cells [20]. nc-SiO_x:H layers in this case not only offer better carrier transport and field effect passivation but also improve carrier selectivity and reduce parasitic absorption [21]. Depending on the application, these layers fulfil various requirements such as: doped layer to build up the electric field in diode, nucleation layer to promote crystalline growth or as an appropriate recombination junction with low series resistance. Therefore, in this work, we discuss the versatility of nanocrystalline silicon oxide (nc-SiOx:H) material deposited by industrial, high throughput plasma enhanced chemical vapor deposition (PECVD) tool for different photovoltaic applications - front contacts, back reflectors, and intermediate window layers. Parameters like concentration of dilution gases, doping gases, RF power, and total pressure are examined in a detailed manner as illustrated in Figure 1a. During the PECVD deposition of nc-SiO_x:H, silane (SiH_4) provides silicon, carbon dioxide (CO_2) supplies oxygen, phosphine (PH_3) introduces phosphorus for doping, and hydrogen (H_2) serves various functions such as influencing film properties and reducing defects. The combination of these precursor gases, along with the plasma environment, allows for the controlled growth of nc-SiOx:H with tailored composition and properties for specific applications in solar cells.

Through this work we explore and try to understand the relationship between the optical and structural properties of n-type nc-SiOx:H films and their ability to passivate the surface of crystalline silicon as systematically illustrated in Figure 1b. It should be noted that passivation quality of nc-SiOx:H films is a critical factor influencing the performance and efficiency of solar cells. For n-type c-Si wafers, passivation is particularly crucial as it helps to minimize the surface recombination of minority carriers, such as holes and nc-SiOx:H films act as passivation layers for the silicon surface. The material properties, including the crystallinity, hydrogen content, and oxygen content, significantly influence these films ability to passivate the surface effectively. The presence of hydrogen is essential for passivation, as it helps in the formation of silicon-hydrogen bonds that can passivate dangling bonds and trap charge carriers. By understanding and controlling the deposition parameters, it is possible to tailor the passivation layer to suit the specific requirements of n-type c-Si wafers in solar cell applications. This paper distinguishes itself from previous studies by placing a pronounced emphasis on passivation properties within the realm of nanocrystalline silicon oxide (nc-SiOx:H) films. While prior research has predominantly examined these films through the lens of optical and structural properties, our work takes a pioneering approach by elevating the significance of passivation. The primary focus revolves around the intentional development of nc-SiOx films endowed with superior passivating properties, aiming to contribute innovative insights to the field of solar cell technology.

Preprints.org (www.preprints.org) | NOT PEER-REVIEWED | Posted: 20 February 2024 doi:10.20944/preprints202402.1053.v1

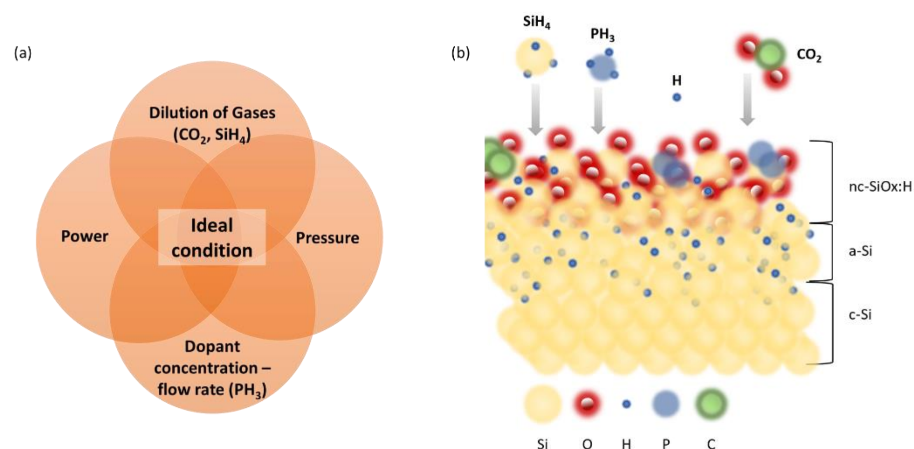

Figure 1. (**a**) Schematic of interdependence of deposition parameters for the growth of doped nc-SiOx:H films by plasma enhanced chemical vapour deposition system (PECVD) studied in this work. (**b**) Pictographic representation of surface growth reaction of nc-SiOx:H structure deposited using silane (SiH_4), hydrogen (H_2), carbon dioxide (CO_2) and phosphine (PH_3) as precursor gases. Each gas has a specific role in determining the composition, structure, and properties of the deposited film. SiH_4 serves as the silicon (Si) precursor whereas CO_2 acts as the oxygen (O) precursor and provide Si and O respectively for the formation of silicon oxide in the PECVD process. The incorporation of hydrogen from SiH_4 can also influence the hydrogenation level in the film, affecting its passivation properties. PH_3 acts as the dopant precursor and introduces phosphorous (P) in the deposited silicon oxide films. The addition of phosphorus can modify the electrical properties of the film, influencing its conductivity or other characteristics.H_2 is commonly used as co-reactant or reducing agent in the PECVD processes (also in our case). Chemical species shown in the image are for representation purposes only (not to scale).

2. Materials and Methods

N-type, nc-SiOx:H layers were deposited in an industrial grade, plasma-enhanced chemical vapor deposition system - PECVD, (IndeoTec Octopus) on 1/4 of 4-inch, n-type FZ c-Si wafers with a resistivity of 1-3 Ω.cm and Corning glass. c-Si wafers were dipped in 5% HF solution for 30 sec to remove the native oxide before introducing them in the PECVD chamber. A mixture of silane (SiH_4), dihydrogen (H_2), and carbon dioxide (CO_2) was used as precursor for the deposition as shown in Figure 2. 1% Phosphine (PH_3) diluted in hydrogen was used for n-type doping. Typical deposition parameters were: a pressure of 2.5 mbar, a substrate temperature of 180°C, a deposition time of 10 min and a radio frequency power of 50 W. The flow rates for gases were as follow - SiH_4 : 2 – 8 sccm, CO_2 : 0 – 4 sccm, and PH_3 : 0.5 – 2 sccm. H_2 flow rate was fixed at 500 sccm for all samples discussed in this manuscript. Furthermore, the radio frequency (RF) plasma power and pressure were varied within 20 W - 80 W and 1.4 Torr - 3 Torr respectively. It should be noted that in all cases a thin layer of a-Si:H was deposited on c-Si wafer at 25 W, 1.6 mbar for 30 sec in order to provide a better passivation of the c-Si before deposition of the nanocrystalline silicon oxide layers. The deposition time was fixed at 10 min. Note that we target thin films (in the range of 10 nm - 45 nm) relevant for passivation layers in solar cells. Thicker layers could be better crystallized but are not useful as too much absorption would happen.

Preprints.org (www.preprints.org) | NOT PEER-REVIEWED | Posted: 20 February 2024 doi:10.20944/preprints202402.1053.v1

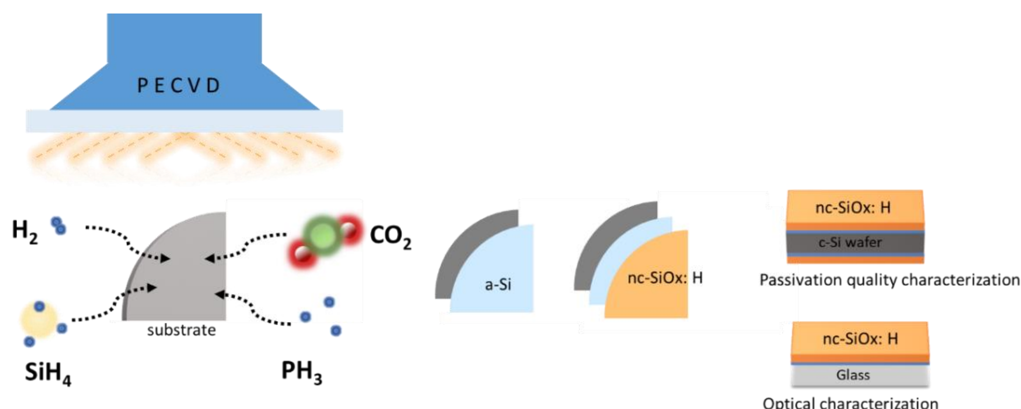

Figure 2. Schematic of experimental process flow for depositing nc-SiOx:H films both on c-Si wafers and Corning glass substrates in the PECVD chamber. A thin buffer layer of a-Si:H was deposited on the substrate before depositing nc-SiOx:H films.

In this work, minority carrier lifetime (τ) is used as a measure of passivation quality because it provides information about the recombination of minority carriers (photocarrier) lifetime at the surface of a semiconductor material. It is composed of the bulk lifetime and surface lifetime, which depend on the surface properties of the sample. In low-level injected material, where the number of minority carriers is less than the doping, the lifetime is determined by the recombination rate (R), expressed as:

$$\tau = \frac{\Delta n}{R}$$

where τ is the minority carrier lifetime, Δn is the excess minority carrier concentration [22]. Longer τ indicates better passivation, suggesting lower recombination rates at the surface. This means there is a higher probability of carriers reaching the electrical contacts before recombining, which contribute to enhanced charge collection efficiency for solar cells. It should be noted that terms 'long lifetime' and 'high lifetime' are used interchangeably when we discuss this. The effective minority carrier lifetime (τ_{eff}) of the symmetrical samples was determined using the QSSPC method in generalized mode using Sinton Lifetime Tester. The reported are as-deposited values extracted at a minority carrier injection level of 10^{15} cm^{-3} as detailed in [23]. Similarly, 1-sun implied open-circuit voltage (iV_{oc}) was also extracted. Thermal annealing was avoided in this study so that an additional step is evaded for industrial compatibility. Subsequently, the homogeneity of the passivation quality was also determined by photoluminescence (PL) images obtained using a BTi luminescence imaging system at 1 sun. Optical properties of the films were measured via spectroscopic ellipsometry (SE) in the spectral range [1.5 eV – 5 eV] using a phase modulated ellipsometer (UVISEL from HORIBA John-Yvon). We measured films on both c-Si and glass substrates. The ellipsometric data were modeled using Bruggeman effective medium approximation (BEMA) using the DeltaPsi2 software on c-Si substrates. The optical gap of the film, denoted by E_{04}, was estimated as the photon energy at which the absorption coefficient is 10^4 cm^{-1}. We used the E_{04} value to provide an estimation of the optical gap because it is simpler and less error prone than the Tauc method. However, if we carefully estimate the Tauc gap of the film, we can easily find a linear relationship between E_{04} and the Tauc gap as used in [24,25]. Raman spectroscopy was used to analyze nanocrystalline and amorphous silicon phases in the films. Raman spectra were obtained with Horiba Raman Microscope in the range of 350 cm^{-1} – 1100 cm^{-1} using a laser with wavelength of 532 nm on silicon samples. Raman spectra of the n-layers deposited on Si samples was used to identify and distinguish the presence of amorphous silicon and crystalline silicon phases in the nc-SiOx:H films. Finally, SEM Images were obtained using a Zeiss instrument (Merlin compact) – at various magnifications and we also used EDX tool to analyze the compositional changes at nanoscale level.

3. Results and Discussion

Preprints.org (www.preprints.org) | NOT PEER-REVIEWED | Posted: 20 February 2024 doi:10.20944/preprints202402.1053.v1

3.1. Optimization of Oxygen Content (CO_2 Series)

CO_2 is used an oxygen precursor in the PECVD process for silicon oxide deposition i.e. it provides oxygen for the formation of the silicon oxide film. The interaction of CO_2 in the plasma generates reactive oxygen species that react with silicon precursors to form silicon oxide bonds. In this set, the CO_2 flow rate was varied from 0-4 sccm in order to determine the optimum deposition conditions for the n-type nc-SiOx:H films. The deposition conditions used for these films were fixed as follows: PH_3 – 0.8 sccm, SiH_4 – 4 sccm, Power – 50W, Pressure – 2.5 Torr. Figure 3. shows the effect of the CO_2 flow rateon the passivation quality provided by nc-SiOx:H films. The CO_2 flow ratio is defined as

$$r_{CO_2} = \frac{f_{CO_2}}{f_{SiH_4} + f_{CO_2}} \times 100$$

where f_{CO_2} and f_{SiH_4} are the CO_2 and SiH_4 gas flow rates respectively. We started with r_{CO_2}= 0% which means we are likely get amorphous Si or nc-Si:H films.

It can be observed that upon introduction of CO_2 gas in the deposition chamber there is an improvement in lifetime, from 879 ± 31 µs to 2412 ± 72 µs. A similar trend was observed on iV_{oc} values as well increasing from 674.5 ± 0.5 mV to 710 ± 1 mV. However, too much CO_2 in the chamber i.e. increasing the gas flow ratio from 33% to 50% results in deterioration of lifetime and the passivation quality of the film (τ_{eff} = 377 ± 5 µs and iV_{oc} = 649 mV).

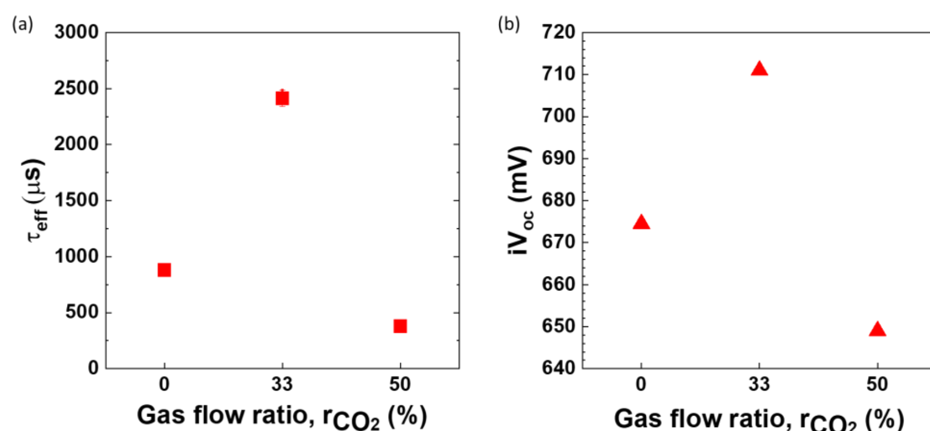

Figure. 3. Variation in (**a**) effective minority carrier lifetime (τ_{eff}), and (**b**) implied open circuit voltage (iV_{oc}) of nc-SiOx:H films deposited with changing CO_2 gas flow ratio. Please note the lifetime curves for these gas ratios can be found in supplementary section Figure S1.

In order to understand the dependence of the effective lifetime on the CO_2 fraction we analyzed the structural properties of the layers. Figure 4. displays the CO_2 gas flow dependence of the material properties of nc-SiOx:H films. EDX spectra show peaks at 0.27 eV, 0.53 eV and 1.742 eV corresponding to carbon, oxygen and silicon respectively. It verifies that increasing the CO_2 flow rate from 0% to 50% results in an augmentation of O content (from 165 counts → 245 counts → 342 counts) but a relative reduction in Si content (10970 counts → 10898 counts →10825 counts) within the films. We also observed an increase in the thickness of the films from 15.7 nm to 31.6 nm with rise in r_{CO_2}. E_{04} values however are in the similar ballpark i.e. 2.16 eV for these samples.

In the plasma, CO_2 splits into O and CO according to the reaction:

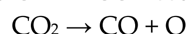

$$CO_2 \rightarrow CO + O$$

As the r_{CO_2} in the deposition chamber increases from 0% to 33%, the presence of CO and O is expected to increase in chamber as well as in the films. According to the etching model of µc:Si:H formation, during the deposition process atomic H reaching the film-growing surface weakens the Si-Si bond in the amorphous network, which can be replaced by a stronger Si-O bonds due to presence of free O atoms/ radicals, and resulting in more likelihood for the of Si-O-Si bond formation.

Das et al. demonstrated that higher concentration of atomic oxygen introduces additional structural defects [12] aiding merit to above hypothesis.

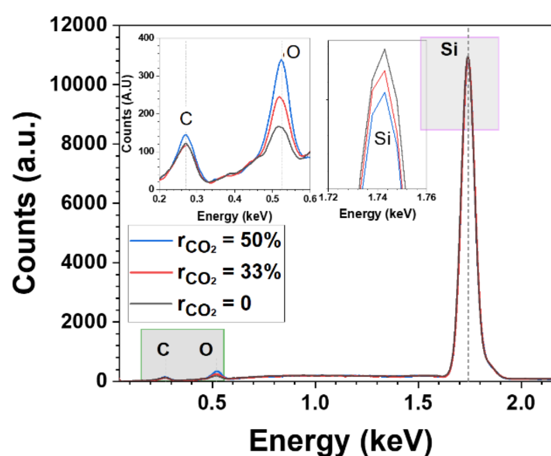

Figure 4. EDX spectra of nc-SiOx:H layers deposited at different CO_2 gas flow ratio. The inset is the magnification of C,O and Si peaks.

When r_{CO_2} is further increased from 33% to 50%, more free oxygen forms stronger bonds with Si, forming more Si-O-Si bonds that are more energetically stable than Si-Si bonds. This reduces the etching potential due to higher hydrogen dilution, which can lead to increased presence of O in the films, thicker layers due to the reduced etching, lower crystallinity, and eventually poor passivation quality as seen in case of r_{CO_2}= 50% in Figure 3. Although most of the C is expected to leave the deposition chamber in the form of CO or CO_2, a small amount is still embedded in the film [26,27]. Even in this case, at r_{CO_2}=50%, C is incorporated in the deposited nc-SiOx:H film (Figure 4) i.e. 144 counts compared to 121 counts in case of r_{CO_2}= 0%. This is could also be a reason for lower crystallinity at r_{CO_2}=50%.

SEM images ((Figure 5a,b) also confirm visually that sample with CO_2 flow rate 33% has more grains than its 50% counterpart. It has also been shown by Das et al. that an increase in CO_2 flow rate leads to decrease in the grain size as well as crystallite size in n type-μc-SiO:H films [12]. This phenomenon is attributed to the elevated partial pressure of CO_2 within the gas mixture, resulting in higher oxygen content in the films. The heightened presence of atomic oxygen introduces extra structural defects, thereby hindering the growth of crystallites and influencing their size [8]. Also, C gets incorporated in these nc-SiOx:H films. On the other hand, Smirnov et al. and Shin et al. illustrated that extremely high O-incorporation in the film can potentially cause an obstruction in the growth of crystallites resulting in a very low dark conductivity [24,28].

The ability to control the O content in nc-SiOx:H films offers a means to tailor their passivation quality and crystallinity, which are critical for enhancing the efficiency of solar cells. By optimizing the O content, it is possible to achieve improved passivation of crystalline silicon wafers, leading to reduced recombination rates at the surface and, consequently, higher τ_{eff}. This, in turn, can enhance the efficiency of carrier extraction in solar cells, ultimately contributing to improved overall device performance. Higher oxygen content (r_{CO_2} = 33%) enhances the passivation quality of films and crystallinity. However, too much oxygen is detrimental for the overall quality of films. This is due to more incorporation of O in the films at even higher r_{CO_2} (50%). Though we obtain thicker films but with lower crystallinity and poor passivation quality. The relationship between the oxygen content, crystallinity, and passivation quality of nc-SiOx:H films is a key factor in the development of advanced solar cell technologies, offering a pathway to enhance the efficiency and performance of solar energy conversion devices. Therefore, it is important to keep in mind the application of these

Preprints.org (www.preprints.org) | NOT PEER-REVIEWED | Posted: 20 February 2024 doi:10.20944/preprints202402.1053.v1

passivating nc-SiOx:H films while deciding the flow rate of CO_2 gas. Since, we are looking at films with high passivation quality, we choose r_{CO_2}=33% for next set of experiments.

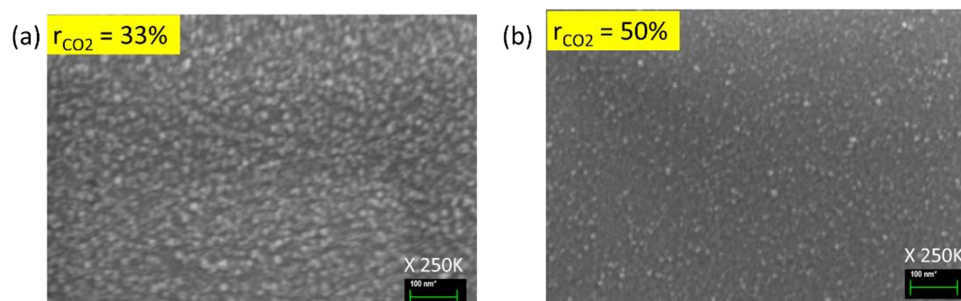

Figure 5. SEM images of nc-SiOx:H films deposited at CO_2 gas flow ratio (**a**) 33% and (**b**) 50% at magnification ratio of 250K.

3.2. Optimization of SiH_4 Series

Moving forward, we will explore the influence of the silane (SiH_4) flow rate on the growth of our nc-SiOx:H films. SiH_4 serves as the silicon precursor i.e. it provides the silicon component for the formation of the silicon oxide films. It undergoes dissociation in the plasma, and the resulting silicon species contribute to the deposition of the silicon oxide film. The incorporation of hydrogen from silane can also influence the hydrogenation level in the film, affecting its passivation. We will be using hydrogen dilution parameter for ease of comparison as most publications report this parameter. However, we also report the results with regards to changing silane flow rate. It is generally understood that a higher hydrogen dilution is necessary to obtain nano-crystalline Si films. The hydrogen dilution ratio is described as R = $[H_2]/[SiH_4]$ and the nature of the grown film depends strongly on this parameter. The deposition conditions used for these films were fixed as follows- CO_2 – 2 sccm, PH_3 – 0.8 sccm, Power – 50 W, Pressure – 2.5 Torr. As far as the passivation properties of the nanocrystalline silicon oxide films are concerned, we observe that upon decreasing the hydrogen dilution, the lifetime increases drastically from 42 µs (R = 250) to 4020 ± 71 µs (R = 62.5) (Figure 6a). Correspondingly, iV_{oc} also mirrors this trend as it rises from 578 mV to 715.5 ± 0.5 mV as shown in Figure 6b. The photoluminescence mapping in Figure 6c shows the effective carrier lifetime is quite homogeneous over the quarter of 4” wafer.

As the silane flow rate increases, we see an increase in thickness of nc-SiOx:H films from 25.4 nm to 40.9 nm and hence deposition rate of films (Figure 7a). The optical gap of films also decreases steadily from 2.33 eV to 2.04 eV with an increase in with SiH_4 flow rate (lower R) as shown in Figure 7.

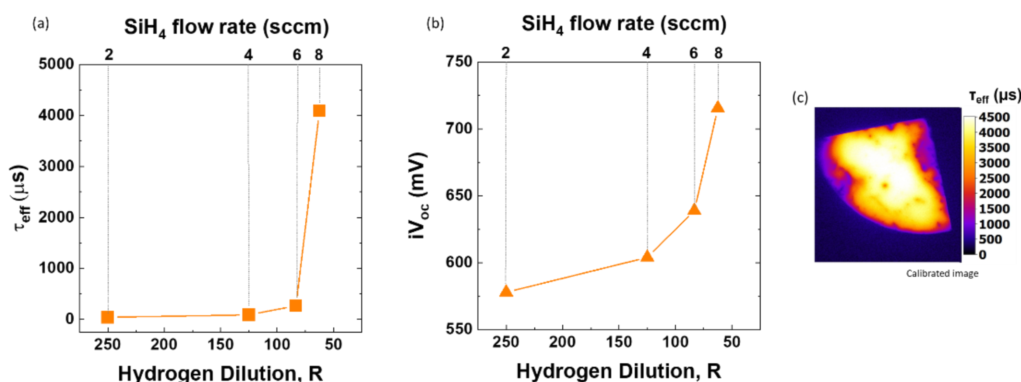

Figure 6. Variation of electrical properties ((**a**) Lifetime (τ_{eff}) and (**b**) Implied open circuit voltage (iV_{oc}) with changing hydrogen dilution (R) i.e. by varying the SiH_4 flow rate from 2 sccm to 8 sccm (**c**) Calibrated PL image of sample deposited at SiH_4 flow rate = 8 sccm (i.e. R=62.5) at steady state light intensity of 1 sun.

Preprints.org (www.preprints.org) | NOT PEER-REVIEWED | Posted: 20 February 2024 doi:10.20944/preprints202402.1053.v1

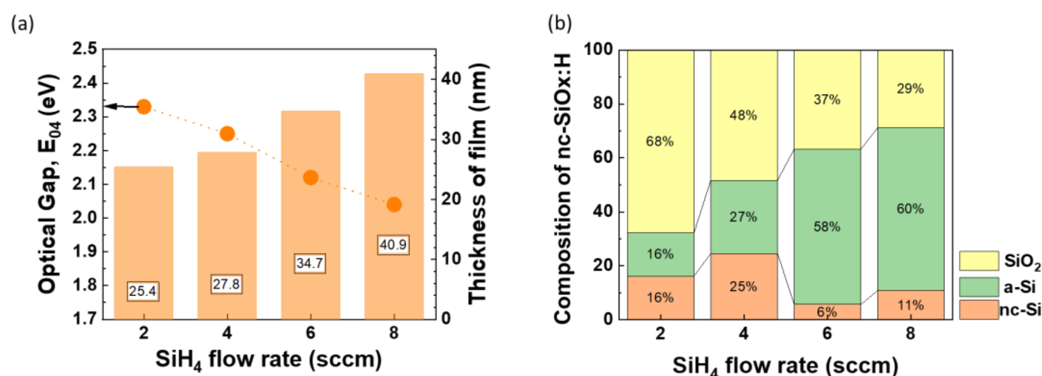

Figure 7. Impact of variation in silane (SiH_4) flow rate (2-8 sccm) on (**a**) Optical Gap (E_{04}) and thickness of films (nm) (**b**) composition of nanocrystalline silicon oxide (nc-SiOx:H) films.

Raman spectra of the films reveal c-Si peak at 520 cm^{-1} as the substrate was c-Si. The broader features observed around 480 cm^{-1}, are attributed to a-Si phase. Films with low silane flow rate (2 sccm and 4 sccm) i.e. higher dilution (high R) shows no presence of a-Si phase. Raman data also illustrates that these nc-SiOx:H films develop amorphous phase when we increase the silane flow rate from 2 sccm to 8 sccm (Figure 8a). The composition of the films obtained from BEMA modelling (Figure 7b) also shows rise in a-Si fraction from 16% to 60% with corresponding surge in flow rate from 2 sccm to 8 sccm. SEM imaging on the 2 sccm sample revealed the existence of very small grains (image not shown). Elemental EDX analysis (Figure 8b) of the nc-SiOx:H films deposited at a SiH_4 flow rate of 4 sccm reveal higher levels of elemental C (148 counts) and O (351 counts) compared to its 8 sccm counterpart (C = 121 counts and O = 214 counts). Figure 7b also indicates the higher presence of SiO_2 phase (4 sccm - 48%, 8 sccm - 29 %) and nc-Si phase (4 sccm - 25%, 8 sccm - 11%) in the 4 sccm sample compared to its 8 sccm counterpart. In contrast for sample with 8 sccm flow rate, a-Si phase is more dominant i.e. 60% compared to 27% (Figure 9). It implies that relatively higher hydrogen dilution is required for achieving better micro crystallinity, whereas low hydrogen dilution is needed for producing amorphous nc-SiOx:H films.

Given high E_{04} values at high R (low SiH_4 flow rate) these films are well suited to be used as back reflector or window layer whereas at low R (high SiH_4 flow rate) films can act as a passivating contact or even recombination layers in solar cells. Since we focus on highly passivating layers, we choose SiH_4 flow rate 8 sccm for the next set.

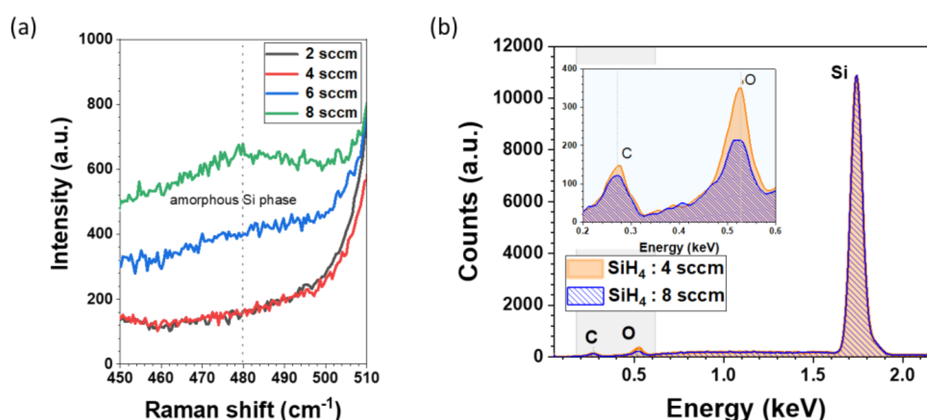

Figure 8. (**a**) Raman spectra of nanocrystalline silicon oxide (nc-SiOx:H) films deposited at varying Silane flow rate (2 – 8 sccm) on c-Si (**b**) EDX elemental analysis of nc-SiOx:H films deposited at silane flow rate of 4 sccm and 8 sccm.

Preprints.org (www.preprints.org) | NOT PEER-REVIEWED | Posted: 20 February 2024 doi:10.20944/preprints202402.1053.v1

3.3. Optimization of RF Power

RF Power is another important parameter that affect the dissociation of precursors and therefore film composition. It is known that at a given set of deposition conditions, an increase in ion energy on the substrate may lead to defects and be potentially harmful to the interface [29]. In contrast, because of the increased surface mobility of reactive species, a sufficiently low level of ion bombardment is deemed to be beneficial for growth. Therefore, it is imperative for us to understand the role of power in determining passivation properties and doping nanocrystalline thin films. The deposition conditions for this set are: CO_2 – 2 sccm, PH_3 – 0.8 sccm, SiH_4 – 8 sccm, Pressure – 2.5 Torr.

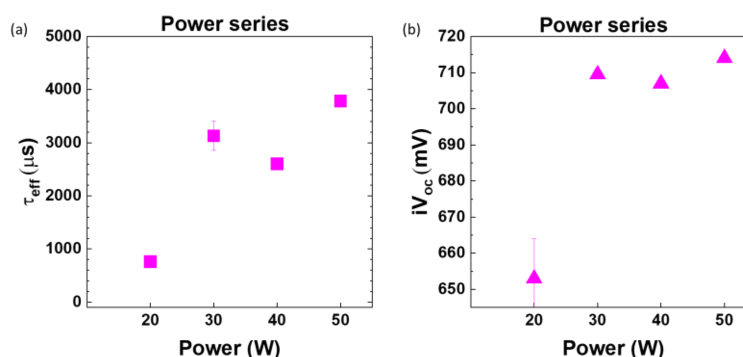

Figure 9. (**a**) Effective minority carrier lifetime (τ_{eff}) and (**b**) implied V_{oc} (iV_{oc}) of nanocrystalline silicon oxide (nc-SiOx:H) films deposited at various powers (20-50 W).

As the RF power is reduced from 50 W to 20 W, a decline in the passivation properties of the films is observed, with a decrease from 3784 ± 99 μs at 50 W to 759 ± 112 μs at 20 W(Figure 9). The lower passivation at 20 W may be attributed to the deposition of films with higher susceptibility to defects within the initial few nanometers of growth at lower power, considering the film's thickness is only 6.4 nm (refer to Figure 10a). Concurrently, iV_{oc} exhibits an increase from 653 ± 11 mV at lower power (20 W) to 714 ± 1 mV when the power is elevated to 50 W. Additional investigations were conducted at power levels exceeding 50 W (specifically, 60 W, 70 W, and 80 W). Nevertheless, the passivation quality, as indicated by both effective lifetime (τ_{eff}) and iV_{oc}, systematically deteriorates beyond 50 W which could be attributed to excessive ion bombardment energy (plot for the same in supplementary section Figure S3).

Figure 10 shows that as we decrease the power from 50 W to 20 W, the optical gap of the films increases from 1.56 eV to 1.96 eV. Moreover, decrease in power also results in a significant drop in crystalline fraction from 54% to 13% accompanied by an increase of a-Si fraction from 24% to 70%. This can be attributed to the fact that at low power H_2 dissociation and H production required for the nucleation of crystallites is not enough. Similar trend has been reported by Juneja et al. based on Raman spectroscopy and SEM images [30].

Higher power promotes the decomposition of silane (SiH_4) and hydrogen (H_2), generating radicals like SiH_x and atomic hydrogen. SiH_3 specifically acts as a film-forming precursor, and atomic hydrogen promotes the nucleation of a crystalline phase and enhances precursor diffusion on the growing surface [31]. It has been reported that higher applied power favors microcrystalline/nanocrystalline growth [24,32].

Preprints.org (www.preprints.org) | NOT PEER-REVIEWED | Posted: 20 February 2024 doi:10.20944/preprints202402.1053.v1

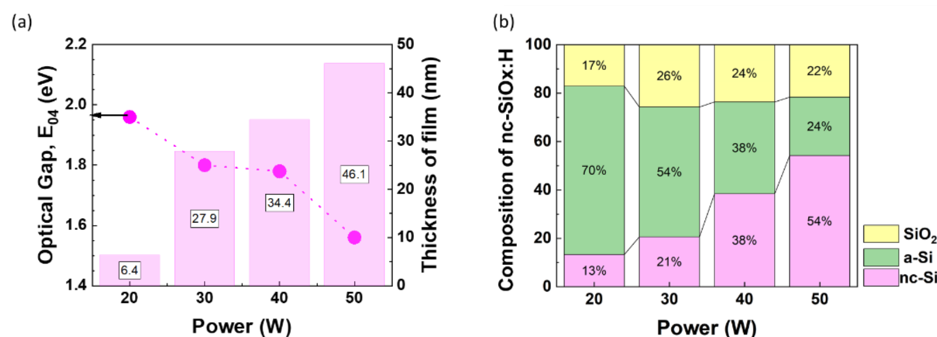

Figure 10. Comparison of nc-SiOx:H films deposited at different power variation (20 – 50 W) (**a**) Optical Gap and thickness of film, (**b**) structural composition of different phases of nc-SiOx:H layers.

Overall optimized power results from a tradeoff between the generation of a high-density plasma and low energy ions which result in deposition of high crystalline structure. In order to form good nanocrystalline silicon oxide films we need good passivation, crystallinity as well as absorption (i.e. high lifetime, high I_c and E_{04} closer to 2 eV). Therefore, we chose a RF power of 30 W for next set.

3.4. Optimization of Total Pressure

The deposition conditions for this set are CO_2: 2 sccm, PH_3 – 0.8 sccm, SiH_4 – 8 sccm, Power – 30 W. Figure 11 clearly shows a positive correlation between pressure and passivation quality provided by nanocrystalline silicon oxide films. Higher chamber pressure results in higher lifetime. For deposition pressure values between 1.4 Torr -1.8 Torr, the passivation quality is rather low (less than 300 µs). It is only at 2 Torr and above that the passivation quality of the samples improves, with the sample deposited at 3 Torr showing the highest passivation quality. However, because some powder formation was observed on the sample at such high pressure we preferred 2.5 Torr for sample deposition.

Figure 12. give us an insight to this. At low chamber pressure (1.4 Torr – 1.8 TTorr), we observe that very thin films (3.3 nm – 7.5 nm) are formed. It is only at 2 Torr the deposition rate of the films takes off resulting in about three times thicker films (~23 nm -27 nm). This is consistent with the low lifetime values as well (Figure 11). It is known that silane dissociation by electron impact and the reaction $H+SiH_4$ = SiH_3+H_2 are the main channels to produce SiH_3 radicals. Below 2 Torr, the deposition rate is attributed to the increase in the dissociation of rate of SiH_4 and H_2. Between 2 and 2.5 Torr as the deposition pressure increase we see a decrease in nc-Si phase from 21.5% to 18.6%. This trend has also been reported in our previous work on p-uSiOx films [33] and independently by Gabriel et al. [34]. This is because the deposition rate due to SiH_3 radical decreases and is dominated by the production of H_3^+ ions and its thermal fluxes according to the equations shown below :

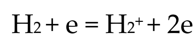
$$H_2 + e = H_2^+ + 2e$$
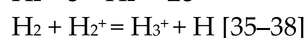
$$H_2 + H_2^+ = H_3^+ + H \quad [35–38]$$

At 3 Torr, we obtain slightly higher E_{04} (2.1 eV) and nc-Si phase (~23.7%). Zhang et al. reported that 2.5 Torr is the critical gas pressure where the ionization of H_2^+ meets the energy threshold, so the production H_3^+ions decreases even though the collision frequency still increases [38]. Therefore, H_2^+ ions production and their thermal fluxes dominate the H_3^+ ions production and their fluxes resulting in higher crystalline fraction and higher disorder.

Preprints.org (www.preprints.org) | NOT PEER-REVIEWED | Posted: 20 February 2024 doi:10.20944/preprints202402.1053.v1

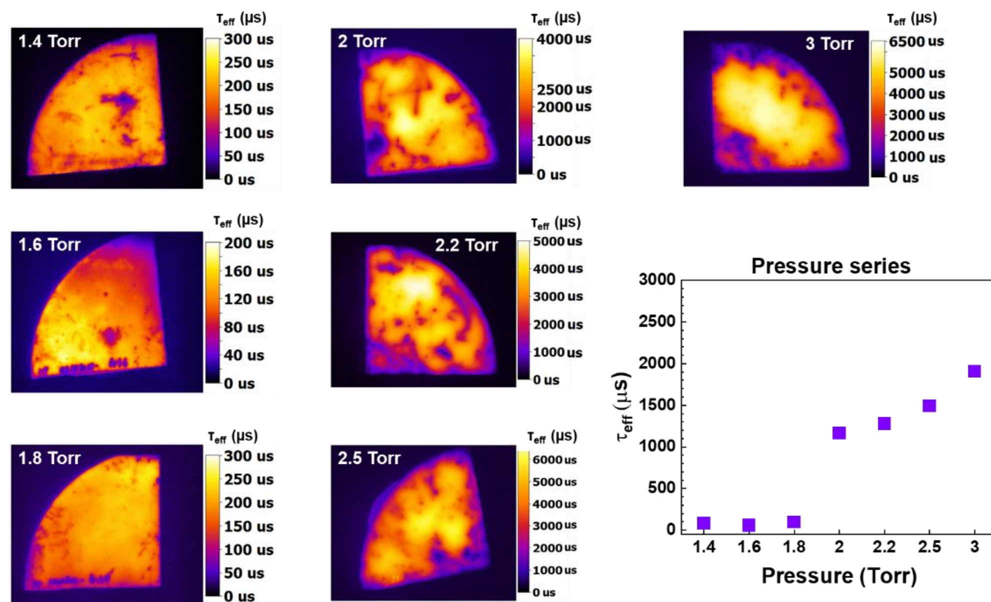

Figure 11. PL image map of nc-SiOx:H films (on Si substrate) deposited at various values of pressure (1.4 Torr - 3 Torr). It is calibrated to minority carrier lifetime (τ_{eff}) at light intensity of 1 sun. Mean value of τ_{eff} from each sample is the also extracted and plotted against each pressure condition.

Therefore, relatively low power (30 W) and high Pressure (2.5 Torr) works best for passivating and crystalline films suitable for even application in silicon heterojunction devices and even perovskite/ silicon tandem solar cells.

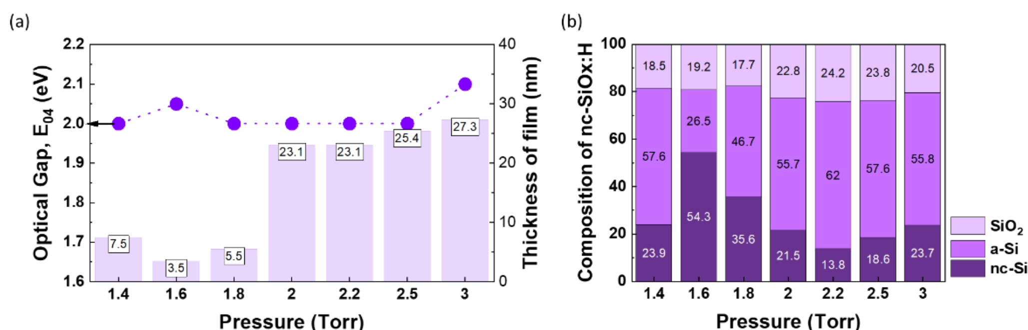

Figure 12. Comparison of nc-SiOx:H films deposited at different pressures (1.4 Torr – 3 Torr) (**a**) Optical Gap and thickness of film, (**b**) structural composition of different phases.

3.5. Optimization of Phosphine Flow Rate (PH_3 Series)

As we know, PH_3 is a dopant precursor, and is used when doping of the nc-SiOx:H film with phosphorus is required. The addition of phosphorus can modify the electrical properties of the film, influencing its conductivity or other characteristics. Therefore, we made films with various values of the phosphine doping ratio by varying PH_3 flow ratio (r_{PH_3})

$$r_{PH_3} = \frac{f_{PH_3}}{f_{SiH_4} + f_{PH_3}} \times 100$$

where f_{PH3} and f_{SiH4} are the PH_3 and SiH_4 gas flow rates respectively. The PH_3 gas was used as a source of phosphor atoms. Please note that PH_3 is diluted at 1% in H_2. The deposition conditions for these films were fixed as follows: CO_2 – 2 sccm, SiH_4 – 8 sccm, Power – 30 W, Pressure : 2.5 Torr. Usually the doping atoms are smaller in number, so it is expected that the crystallinity of the deposited film will not change significantly with the addition of PH_3. However, we do see a change in the passivation quality of the films. Figure 13 shows that upon increasing the flow of PH_3 gas an increase in the

Preprints.org (www.preprints.org) | NOT PEER-REVIEWED | Posted: 20 February 2024 doi:10.20944/preprints202402.1053.v1

passivation quality. τ_{eff} improves from 1673 µs for r_{PH_3}= 6% to 2721 µs for r_{PH_3}= 20% and iV_{oc} follows a similar trend, which can be related to an increased field effect passivation. For r_{PH_3} 20% iV_{oc} of 697 mV is observed. It should be noted that overall a uniform passivation with a lifetime in the range of 3.5 ms can be observed on the sample with r_{PH_3} 20% as shown by PL imaging in Figure 14.

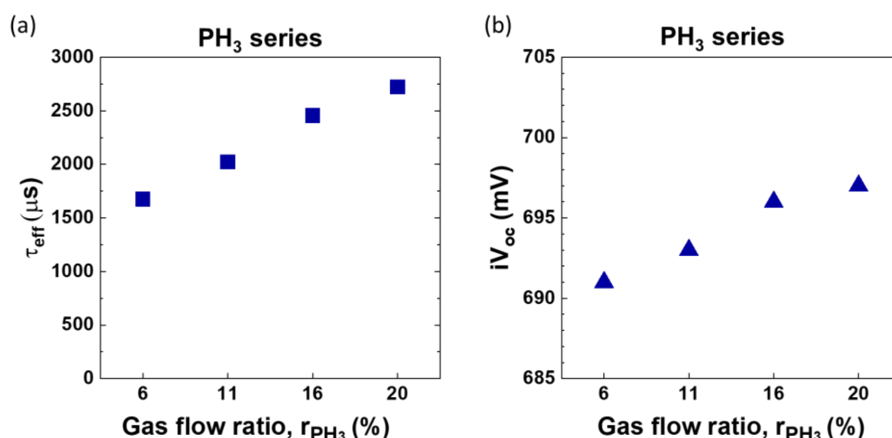

Figure 13. Variation in (**a**) minority carrier lifetime and (**b**) implied V_{oc} with change in gas flow ratio of PH_3. Please note the lifetime curves for these gas ratios can be found in supplementary section Figure S2.

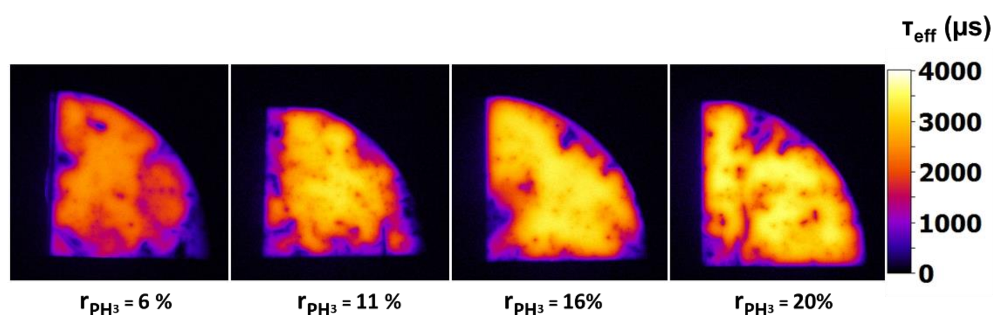

Figure 14. PL Image of nc-SiOx:H samples deposited at different values of the PH_3 gas flow ratio r_{PH_3}= 6%, 11%, 16% and 20%. It is calibrated to lifetime at 1 sun.

The adaptability of hydrogenated nanocrystalline (nc-SiOx:H) material deposited by industrial, high throughput PECVD for photovoltaic applications has been discussed in this work. In addition to talking about how pressure, power, and precursor gases (SiH_4, CO_2, and PH_3) affect the optical and structural characteristics of deposited nc-SiOx:H films, we also emphasized on the significance of passivation qualities when tailoring their development. These n-type nc-SiOx:H films have tunable optical gap range of 1.8 - 2.3 eV and the excellent passivation properties (τ_{eff} up to 4.1 ms, iV_{oc} ~ 715.5 mV) achieved before annealing. Bearing in mind different applications such as front contacts, back reflectors, and intermediate window layers, it is evident that for application of n-type, nc-SiOx:H films in solar cells, there is a trade-off between electrical (τ_{eff} and iV_{oc}), structural (crystalline fraction) and optical properties (Optical Gap, E_{04}). While nc-SiOx:H films with high E_{04} are favorable for window layers or intermediate reflector as their passivation properties are poor. On the contrary, films with high passivation properties and low E_{04} are more suited for front contact or even recombination junction layers in tandem solar cells. r_{CO_2} is a convenient parameter to vary the microstructure as well passivation and optical properties of these films given the role oxygen plays in controlling the defect structure and absorption in the films. Both RF power and pressure play an important role in determining the crystalline fraction of the films and control the amorphous and crystallite phases. Relatively low power (30 W) and high Pressure (2.5 Torr) works best for

Preprints.org (www.preprints.org) | NOT PEER-REVIEWED | Posted: 20 February 2024 doi:10.20944/preprints202402.1053.v1

passivating and crystalline films suitable for application in silicon heterojunction devices and even perovskite/ silicon tandem solar cells. Our results suggest that properties of doped nc-SiOx:H films can be conveniently adjusted to fulfil various requirements as a front contact, intermediate layer and back reflector.

Further, here are practical insights based on our work that researchers and industry professionals can use to tailor the development n-type nc-SiOx:H layers to meet the specific requirements of different solar cell applications:

- Fine-tune the r_{CO_2} ratio to achieve the desired balance between passivation quality and crystallinity, considering the specific requirements of the solar cell application.
- Controlling the dilution rate (R) during deposition allows tuning the hydrogen content in the film for effective passivation
- Tailor the r_{PH_3} to achieve the desired doping level for specific solar cell designs, ensuring optimal passivation properties without introducing excessive defects.
- Choose an appropriate plasma property (power and pressure) based on the desired balance between crystallinity and passivation.

4. Conclusions

This work focused on optimizing the deposition conditions for nanocrystalline silicon oxide (nc-SiOx:H) films, aiming at enhancing their potential for applications in silicon heterojunction devices and tandem cells. The study systematically explored various deposition parameters, including carbon dioxide (CO_2) flow, silane (SiH_4) flow, RF power, total pressure, and phosphine (PH_3) doping, to understand their individual and collective impacts on film properties. In the investigation of CO_2 flow, it was observed that a 33% CO_2 flow ratio positively influenced minority carrier lifetime (τ_{eff} = 2412 ± 27.5 μs) and open circuit voltage (iV_{oc} = 711 ± 1 mV), indicating improved passivation quality. However, increasing the CO_2 flow ratio to 50% resulted in a decline in both τ_{eff} and iV_{oc}, suggesting a delicate balance. The introduction of atomic oxygen from CO_2 influenced film morphology and composition, impacting crystallite growth and overall passivation quality. Silane (SiH_4) flow was then studied, revealing that higher hydrogen dilution (lower R values) led to a transition from microcrystalline to amorphous phases. An increase in SiH_4 flow (8 sccm) resulted in lower oxygen incorporation, as indicated by a decrease in the optical gap (2.04 eV). This sample also showed τ_{eff} as high as 4.1 ms (iV_{oc} = 715.5 mV) before annealing. Raman spectra supported these findings, showing shifts in crystalline and amorphous phases. Power optimization was explored, highlighting that power in the range of 30-50 W struck a balance between passivation, crystallinity, and absorption. Films deposited at medium powers exhibited better passivation properties, while powers above 50 W led to increased defects and lower crystallinity. Pressure variation demonstrated a positive correlation between higher pressure and improved passivation quality. Films deposited at 2.5 Torr showed the best properties, indicating the importance of deposition conditions in achieving optimal film characteristics. Lastly, phosphine (PH_3) doping was investigated, showing that increasing PH_3 flow rates improved passivation quality, as seen in increased τ_{eff} and iV_{oc}, probably related to enhanced field effect passivation. Overall, the optimal deposition conditions were identified as a 33% CO_2 flow ratio, 8 sccm SiH_4 flow, 30 W power, 2.5 Torr pressure, and 20% PH_3 flow ratio for doping. These conditions aim to strike a balance between passivation quality, crystallinity, and absorption for potential applications in solar cell technology. Further studies on conductivity and crystalline volume fraction are suggested for a more comprehensive understanding of material properties and practical applications in solar cell technology. Overall, this research contributes valuable insights to the ongoing development of efficient thin-film solar cell technology.

Author Contributions: Conceptualization: Gurleen Kaur and Pere Roca i Cabarrocas; methodology and experiment design : Gurleen Kaur; data collection and analysis: Gurleen Kaur and Antonio J. Olivares, software analysis: Gurleen Kaur and Antonio J. Olivares; validation: Gurleen Kaur, Pere Roca i Cabarrocas; writing—original draft preparation: Gurleen Kaur.;

Preprints.org (www.preprints.org) | NOT PEER-REVIEWED | Posted: 20 February 2024 doi:10.20944/preprints202402.1053.v1

writing—review and editing : Gurleen Kaur, Antonio J. Olivares, Pere Roca i Cabarrocas; visualization, Gurleen Kaur; supervision: Pere Roca i Cabarrocas; project administration: Pere Roca i Cabarrocas; funding acquisition: Pere Roca i Cabarrocas. All authors have read and agreed to the published version of the manuscript.

Funding: This work was partially funded by the SOLAR-ERA.NET project "CUSTCO" ANR-19-SOL2-0002-04 of the French Research National Agency (ANR) as well as by the French Government in the frame of the program of investment for the future (Programme d'Investissement d'Avenir - ANR-IEED-002-01)

Acknowledgments: Authors would like to thanks funding by Institut Photovoltaïque d'Ile-de-France (IPVF) and Laboratoire de Physique des Interfaces et des Couches Minces (LPICM) for their support.

Conflicts of Interest: The authors declare no conflicts of interest.

References

1. L. Mazzarella, A. Morales-Vilches, L. Korte, R. Schlatmann, and B. Stannowski, 'Versatility of Nanocrystalline Silicon Films: from Thin-Film to Perovskite/c-Si Tandem Solar Cell Applications', *Coatings*, vol. 10, no. 8, p. 759, Aug. 2020, doi: 10.3390/coatings10080759.
2. P. Cuony *et al.*, 'Mixed-phase p-type silicon oxide containing silicon nanocrystals and its role in thin-film silicon solar cells', *Appl. Phys. Lett.*, vol. 97, no. 21, p. 213502, Nov. 2010, doi: 10.1063/1.3517492.
3. P. Cuony *et al.*, 'Silicon Filaments in Silicon Oxide for Next-Generation Photovoltaics', *Adv. Mater.*, vol. 24, no. 9, pp. 1182–1186, Mar. 2012, doi: 10.1002/adma.201104578.
4. K. Ding, U. Aeberhard, V. Smirnov, B. Holländer, F. Finger, and U. Rau, 'Wide Gap Microcrystalline Silicon Oxide Emitter for a-SiO_x:H/c-Si Heterojunction Solar Cells', *Jpn. J. Appl. Phys.*, vol. 52, no. 12R, p. 122304, Dec. 2013, doi: 10.7567/JJAP.52.122304.
5. K. Ding *et al.*, 'Impact of doped microcrystalline silicon oxide layers on crystalline silicon surface passivation', *Can. J. Phys.*, vol. 92, no. 7/8, pp. 758–762, Jul. 2014, doi: 10.1139/cjp-2013-0627.
6. A. Lambertz, T. Grundler, and F. Finger, 'Hydrogenated amorphous silicon oxide containing a microcrystalline silicon phase and usage as an intermediate reflector in thin-film silicon solar cells', *J. Appl. Phys.*, vol. 109, no. 11, p. 113109, Jun. 2011, doi: 10.1063/1.3592208.
7. A. Lambertz, 'Development of Doped Microcrystalline Silicon Oxide andits Application to Thin-Film Silicon Solar Cells', University Utrecht, 2015. Accessed: Jun. 09, 2023. [Online]. Available: https://juser.fz-juelich.de/record/190115/export/he?ln=en
8. A. Richter, V. Smirnov, A. Lambertz, K. Nomoto, K. Welter, and K. Ding, 'Versatility of doped nanocrystalline silicon oxide for applications in silicon thin-film and heterojunction solar cells', *Sol. Energy Mater. Sol. Cells*, vol. 174, pp. 196–201, Jan. 2018, doi: 10.1016/j.solmat.2017.08.035.
9. V. Smirnov, W. Böttler, A. Lambertz, H. Wang, R. Carius, and F. Finger, 'Microcrystalline silicon n-i-p solar cells prepared with microcrystalline silicon oxide (μc-SiO_x:H) n-layer', *Phys. Status Solidi C*, vol. 7, no. 3–4, pp. 1053–1056, Apr. 2010, doi: 10.1002/pssc.200982830.
10. V. Smirnov, A. Lambertz, B. Grootoonk, R. Carius, and F. Finger, 'Microcrystalline silicon oxide (μc-SiOx:H) alloys: A versatile material for application in thin film silicon single and tandem junction solar cells', *J. Non-Cryst. Solids*, vol. 358, no. 17, pp. 1954–1957, Sep. 2012, doi: 10.1016/j.jnoncrysol.2011.12.019.
11. V. Smirnov, W. Boettler, A. Lambertz, O. Astakhov, R. Carius, and F. Finger, 'N-type Microcrystalline Silicon Oxide (μc-SiO_x:H) Window Layers with Combined Anti-reflection Effects for n-i-p Thin Film Silicon Solar Cells', *MRS Proc.*, vol. 1245, pp. 1245-A21-02, 2010, doi: 10.1557/PROC-1245-A21-02.
12. G. Das *et al.*, 'Development of n-type microcrystalline SiOx:H films and its application by innovative way to improve the performance of single junction μc-Si:H solar cell', *J. Mater. Sci. Mater. Electron.*, vol. 28, no. 8, pp. 5746–5753, Apr. 2017, doi: 10.1007/s10854-016-6246-y.
13. L. Mazzarella *et al.*, 'Nanocrystalline n-Type Silicon Oxide Front Contacts for Silicon Heterojunction Solar Cells: Photocurrent Enhancement on Planar and Textured Substrates', *IEEE J. Photovolt.*, vol. 8, no. 1, pp. 70–78, Jan. 2018, doi: 10.1109/JPHOTOV.2017.2770164.
14. A. J. Olivares *et al.*, 'Highly conductive p-type nc-SiOX:H thin films deposited at 130°C via efficient incorporation of plasma synthesized silicon nanocrystals and their application in SHJ solar cells', *Sol. Energy Mater. Sol. Cells*, vol. 266, p. 112675, Mar. 2024, doi: 10.1016/j.solmat.2023.112675.
15. L. Mazzarella, A. B. Morales-Vilches, L. Korte, R. Schlatmann, and B. Stannowski, 'Ultra-thin nanocrystalline n-type silicon oxide front contact layers for rear-emitter silicon heterojunction solar cells', *Sol. Energy Mater. Sol. Cells*, vol. 179, pp. 386–391, Jun. 2018, doi: 10.1016/j.solmat.2018.01.034.

Preprints.org (www.preprints.org) | NOT PEER-REVIEWED | Posted: 20 February 2024 doi:10.20944/preprints202402.1053.v1

16. D. Qiu *et al.*, 'Front contact optimization for rear-junction SHJ solar cells with ultra-thin n-type nanocrystalline silicon oxide', *Sol. Energy Mater. Sol. Cells*, vol. 209, p. 110471, Jun. 2020, doi: 10.1016/j.solmat.2020.110471.
17. V. Smirnov, A. Lambertz, S. Tillmanns, and F. Finger, 'p- and n-type microcrystalline silicon oxide (μc-SiOx:H) for applications in thin film silicon tandem solar cells', *Can. J. Phys.*, vol. 92, no. 7/8, pp. 932–935, Jul. 2014, doi: 10.1139/cjp-2013-0640.
18. M. Q. Khokhar, S. Chowdhury, D. P. Pham, S. Q. Hussain, E.-C. Cho, and J. Yi, 'Improving passivation properties using a nano-crystalline silicon oxide layer for high-efficiency TOPCon cells', *Infrared Phys. Technol.*, vol. 115, p. 103723, Jun. 2021, doi: 10.1016/j.infrared.2021.103723.
19. G. Kaur, Z. Xin, T. Dutta, R. Sridharan, R. Stangl, and A. Danner, 'Improved silicon oxide/polysilicon passivated contacts for high efficiency solar cells via optimized tunnel layer annealing', *Sol. Energy Mater. Sol. Cells*, vol. 217, p. 110720, Nov. 2020, doi: 10.1016/j.solmat.2020.110720.
20. L. Mazzarella *et al.*, 'Infrared photocurrent management in monolithic perovskite/silicon heterojunction tandem solar cells by using a nanocrystalline silicon oxide interlayer', *Opt. Express*, vol. 26, no. 10, pp. A487–A497, May 2018, doi: 10.1364/OE.26.00A487.
21. K. Jäger, J. Sutter, M. Hammerschmidt, P.-I. Schneider, and C. Becker, 'Prospects of light management in perovskite/silicon tandem solar cells', *Nanophotonics*, vol. 10, no. 8, pp. 1991–2000, Jun. 2020, doi: 10.1515/nanoph-2020-0674.
22. R. A. Sinton and R. M. Swanson, 'Recombination in highly injected silicon', *IEEE Trans. Electron Devices*, vol. 34, no. 6, pp. 1380–1389, Jun. 1987, doi: 10.1109/T-ED.1987.23095.
23. G. Kaur *et al.*, 'Understanding Surface Treatment and ALD AlOx Thickness Induced Surface Passivation Quality of c-Si Cz Wafers', *IEEE J. Photovolt.*, vol. 7, no. 5, pp. 1224–1235, Sep. 2017, doi: 10.1109/JPHOTOV.2017.2717040.
24. C. Shin *et al.*, 'Development of highly conducting n-type micro-crystalline silicon oxide thin film and its application in high efficiency amorphous silicon solar cell', *Mater. Sci. Semicond. Process.*, vol. 66, pp. 223–231, Aug. 2017, doi: 10.1016/j.mssp.2017.05.002.
25. S. C. Saha and S. Ray, 'Development of highly conductive n-type μc-Si:H films at low power for device applications', *J. Appl. Phys.*, vol. 78, no. 9, pp. 5713–5720, Nov. 1995, doi: 10.1063/1.359631.
26. A. Richter, V. Smirnov, A. Lambertz, K. Nomoto, K. Welter, and K. Ding, 'Versatility of doped nanocrystalline silicon oxide for applications in silicon thin-film and heterojunction solar cells', *Sol. Energy Mater. Sol. Cells*, vol. 174, pp. 196–201, Jan. 2018, doi: 10.1016/j.solmat.2017.08.035.
27. S. M. Iftiquar, 'The roles of deposition pressure and rf power in opto-electronic properties of a-SiO:H films', *J. Phys. Appl. Phys.*, vol. 31, no. 14, pp. 1630–1641, Jul. 1998, doi: 10.1088/0022-3727/31/14/004.
28. V. Smirnov, A. Lambertz, and F. Finger, 'Electronic and Structural Properties of N-Type Microcrystalline Silicon Oxide (Mc-Siox:H) Films for Applications in Thin Film Silicon Solar Cells', *Energy Procedia*, vol. 84, pp. 71–77, Dec. 2015, doi: 10.1016/j.egypro.2015.12.297.
29. B. Bruneau *et al.*, 'Ion Energy Threshold in Low-Temperature Silicon Epitaxy for Thin-Film Crystalline Photovoltaics', *IEEE J. Photovolt.*, vol. 4, no. 6, pp. 1361–1367, Nov. 2014, doi: 10.1109/JPHOTOV.2014.2357256.
30. S. Juneja and S. Kumar, 'Effect of Power on Crystallinity and Opto-Electronic Properties of Silicon Thin Films Grown Using VHF PECVD Process', *Silicon*, vol. 13, no. 11, pp. 3927–3940, Nov. 2021, doi: 10.1007/s12633-020-00697-7.
31. N. Layadi, P. Roca I Cabarrocas, B. Drévillon, and I. Solomon, 'Real-time spectroscopic ellipsometry study of the growth of amorphous and microcrystalline silicon thin films prepared by alternating silicon deposition and hydrogen plasma treatment', *Phys. Rev. B*, vol. 52, no. 7, pp. 5136–5143, Aug. 1995, doi: 10.1103/PhysRevB.52.5136.
32. H. P. Zhou *et al.*, 'A comparative study on the direct deposition of μc-Si:H and plasma-induced recrystallization of a-Si:H: Insight into Si crystallization in a high-density plasma', *Appl. Surf. Sci.*, vol. 433, pp. 285–291, Mar. 2018, doi: 10.1016/j.apsusc.2017.10.013.
33. A. Olivares Vargas, G. Kaur, M. Poplawski, A. Desthieux, and P. Cabarrocas, 'Optimization of the Conductivity and Crystalline Fraction of p-Type μc-SiOx:H Films for Silicon Heterojunction Solar Cells', in *Optimization of the Conductivity and Crystalline Fraction of p-Type μc-SiOx:H Films for Silicon Heterojunction Solar Cells*, EUPVSEC Proceedings, Nov. 2021, pp. 212–216. doi: 10.4229/EUPVSEC20212021-2EO.3.5.
34. O. Gabriel, S. Kirner, M. Klingsporn, F. Friedrich, B. Stannowski, and R. Schlatmann, 'On the Plasma Chemistry During Plasma Enhanced Chemical Vapor Deposition of Microcrystalline Silicon Oxides', *Plasma Process. Polym.*, vol. 12, no. 1, pp. 82–91, 2015, doi: 10.1002/ppap.201400114.
35. R. K. Janev, W. D. Langer, D. E. Post, and K. Evans, 'Collision Processes and Reaction of H2+Ions', in *Elementary Processes in Hydrogen-Helium Plasmas: Cross Sections and Reaction Rate Coefficients*, R. K. Janev, W. D. Langer, D. E. Post, and K. Evans, Eds., in Springer Series on Atoms+Plasmas. , Berlin, Heidelberg: Springer, 1987, pp. 167–179. doi: 10.1007/978-3-642-71935-6_4.

Preprints.org (www.preprints.org) | NOT PEER-REVIEWED | Posted: 20 February 2024 doi:10.20944/preprints202402.1053.v1

36. M. E. Coltrin, R. J. Kee, and J. A. Miller, 'A Mathematical Model of Silicon Chemical Vapor Deposition: Further Refinements and the Effects of Thermal Diffusion', *J. Electrochem. Soc.*, vol. 133, no. 6, p. 1206, Jun. 1986, doi: 10.1149/1.2108820.
37. K. Landheer, W. J. Goedheer, I. Poulios, R. E. I. Schropp, and J. K. Rath, 'Chemical sputtering by H2+ and H3+ ions during silicon deposition', *J. Appl. Phys.*, vol. 120, no. 5, p. 053304, Aug. 2016, doi: 10.1063/1.4960351.
38. T. Zhang, J.-M. Orlac'h, M. Ghosh, V. Giovangigli, P. R. i Cabarrocas, and T. Novikova, 'Role of H3+ ions in deposition of silicon thin films from SiH4/H2 discharges: modeling and experiments', *Plasma Sources Sci. Technol.*, vol. 30, no. 7, p. 075024, Jul. 2021, doi: 10.1088/1361-6595/ac0da2.

Disclaimer/Publisher's Note: The statements, opinions and data contained in all publications are solely those of the individual author(s) and contributor(s) and not of MDPI and/or the editor(s). MDPI and/or the editor(s) disclaim responsibility for any injury to people or property resulting from any ideas, methods, instructions or products referred to in the content.